J. Fluid Mech. (1993), *vol.* 246, *pp.* 569–591

Determination of two-dimensional magnetostatic equilibria and analogous Euler flows

By D. LINARDATOS

Department of Applied Mathematics and Theoretical Physics, University of Cambridge, Silver Street, Cambridge CB3 9EW, UK

(Received 21 May 1992 and in revised form 14 August 1992)

The equivalence of the method of magnetic relaxation to a variational problem with an infinity of constraints is established. This variational problem is solved in principle and approximations to the exact solution are compared to results obtained by numerical relaxation of fields with a single stationary elliptic point. In the case of a finite energy field of the above topology extending to infinity, we show that the minimum energy state is the one in which all field lines are concentric circles and that this state is topologically accessible from the original one. This state is used as a reference state for understanding the relaxation of fields constrained by finite boundaries. We then consider the relaxation of fields containing saddle points and confirm the tendency of the saddle points to collapse and form two Y-points. An infinite family of local equilibrium solutions each describing a Y-point is provided.

1. Introduction

A method for the determination of a wide family of steady rotational solutions of the Euler equations was suggested by Arnol'd (1974)†, and later developed by Moffatt (1985). This method exploits the well-known exact analogy between steady Euler flows and magnetostatic equilibria in a perfectly conducting fluid, and uses a technique of magnetic relaxation to a (minimum energy) magnetostatic state. The analogy implies that the results derived in this paper apply equally to magnetostatic fields or Euler flows. The proposed method has been implemented for certain two-dimensional configurations by Bajer (1989) who has demonstrated the tendency for the formation of tangential discontinuities of field due to collapse of saddle points (see also the discussion of Moffatt 1990, §8). In the present paper, we develop a modified computational procedure with an improved time-stepping algorithm for two-dimensional magnetic relaxation, and we use this to determine a family of flows in a closed (square) domain with a single elliptic stagnation point. We also study saddle point collapse, and confirm the tendency to form discontinuities in the manner described by Bajer.

Let us consider an incompressible fluid ($\nabla\cdot\boldsymbol{u}=0$) which is contained in a domain $\mathscr{D}$ with boundary $\partial\mathscr{D}$ on which $\boldsymbol{u}\cdot\boldsymbol{n}=0$. Assume further that the fluid is perfectly conducting and that a magnetic field $\boldsymbol{B}(\boldsymbol{x},t)$ satisfying $\nabla\cdot\boldsymbol{B}=0$ and

$$\boldsymbol{B}\cdot\boldsymbol{n}=0 \quad \text{on} \quad \partial\mathscr{D} \tag{1.1}$$

is embedded in it. Condition (1.1) persists under evolution described by the frozen field equation. The magnetic energy of this field is given by

† Arnol'd attributes the conception of this method to Ya. B. Zel'dovich.

$$M(t) = \frac{1}{2}\int_{\mathscr{D}} \boldsymbol{B}^2 \,\mathrm{d}V \tag{1.2}$$

and this changes according to the equation

$$\frac{\mathrm{d}M}{\mathrm{d}t} = \int_{\mathscr{D}} \boldsymbol{B}\cdot\boldsymbol{\nabla}\wedge(\boldsymbol{u}\wedge\boldsymbol{B})\,\mathrm{d}V = -\int_{\mathscr{D}} \boldsymbol{u}\cdot(\boldsymbol{j}\wedge\boldsymbol{B})\,\mathrm{d}V, \tag{1.3}$$

where $\boldsymbol{j} = \boldsymbol{\nabla}\wedge\boldsymbol{B}$. The objective is to adopt the simplest possible equation of motion for the fluid. This equation must incorporate the Lorentz force $\boldsymbol{j}\wedge\boldsymbol{B}$ per unit volume, must allow $\boldsymbol{u}(\boldsymbol{x},t)$ to be incompressible and must further include a term which will dissipate energy. Such an equation of motion is

$$\partial\boldsymbol{u}/\partial t = -\boldsymbol{\nabla}p + \boldsymbol{j}\wedge\boldsymbol{B} - k\boldsymbol{u}, \tag{1.4}$$

where $k > 0$ and $p(\boldsymbol{x},t)$ is the pressure field satisfying

$$\boldsymbol{\nabla}^2 p = \boldsymbol{\nabla}\cdot(\boldsymbol{j}\wedge\boldsymbol{B}) \quad \text{in} \quad \mathscr{D},$$
$$\partial p/\partial n = \boldsymbol{n}\cdot(\boldsymbol{j}\wedge\boldsymbol{B}) \quad \text{on} \quad \partial\mathscr{D}.$$

If $K(t) = \frac{1}{2}\int_{\mathscr{D}} \boldsymbol{u}^2\,\mathrm{d}V$ is the kinetic energy of the flow then

$$\frac{\mathrm{d}K}{\mathrm{d}t} = \int_{\mathscr{D}} \boldsymbol{u}\cdot(\boldsymbol{j}\wedge\boldsymbol{B})\,\mathrm{d}V - 2kK \tag{1.5}$$

so that from (1.3) and (1.5)

$$\frac{\mathrm{d}}{\mathrm{d}t}(M(t)+K(t)) = -2kK. \tag{1.6}$$

Hence for as long as $K(t) > 0$ the total energy $M+K$ is monotonically decreasing and, being positive, must tend to a limit. Dropping the $\partial\boldsymbol{u}/\partial t$ term in (1.4) is equivalent to assuming an instantaneous velocity field. The energy balance then becomes

$$\frac{\mathrm{d}M}{\mathrm{d}t} = -2kK \tag{1.7}$$

and it seems plausible to expect that, whatever the initial conditions,

$$\left.\begin{array}{l} K(t)\to 0 \\ M(t)\to M^{(\mathrm{E})}\ \text{const.} \end{array}\right\} \quad \text{as} \quad t\to\infty. \tag{1.8}$$

Suppose that the initial conditions are

$$\boldsymbol{B}(\boldsymbol{x},0) = \boldsymbol{B}_0(\boldsymbol{x}). \tag{1.9}$$

The initial Lorentz force $(\boldsymbol{\nabla}\wedge\boldsymbol{B}_0)\wedge\boldsymbol{B}_0$ will in general not be irrotational and the pressure forces will not be able to balance it, hence motion will ensue. For all finite time t the flow $\boldsymbol{u}(\boldsymbol{x},t)$ remains smooth and the field $\boldsymbol{B}$ is convected through topologically equivalent states. As $t\to\infty$ though, the volume-preserving mapping induced by $\boldsymbol{u}(\boldsymbol{x},t)$ may develop discontinuities (in the manner described by Moffatt 1985) and consequently the convected field may develop singularities although the total magnetic energy is bounded above by its initial value. For a non-trivial topology the final magnetic energy is also bounded below and away from zero (Arnol'd 1974; Freedman 1988).

An initial field $\boldsymbol{B}_0$, therefore relaxes to a non-trivial equilibrium state $\boldsymbol{B}^{\mathrm{E}}$ which is topologically accessible from $\boldsymbol{B}_0(\boldsymbol{x})$. This means that $\boldsymbol{B}_0(\boldsymbol{x})$ is convected to $\boldsymbol{B}^{\mathrm{E}}(\boldsymbol{x})$ by a smooth incompressible flow $\boldsymbol{u}(\boldsymbol{x},t)$ $(0\leqslant t\leqslant\infty)$ which dissipates a fraction of the

initial magnetic energy. It should be noted that for most fields there may be more than one equilibrium state although in general only one of them will have the least energy.

Boyd & Ma (1990) investigated flows describing a solitary pair of contra-rotating vortices (usually named a *modon*), with the flow in the modon's exterior being irrotational. By prescribing the modon's shape (which they chose to be elliptical) they computed the relationship between the vorticity and the stream function of the rotational flow using a spectral method. In the frame moving with the modon (in which $\boldsymbol{u} \to 0$ as $|\boldsymbol{x}| \to \infty$) the flow in its interior is a steady Euler flow. In the present paper we similarly prescribe the boundary shape and the topology of the initial magnetic field but then allow it to relax dynamically to a magnetostatic equilibrium state. By virtue of the exact analogy between steady Euler flows and magnetostatic equilibria in a perfectly conducting fluid, the equilibrium magnetic field also describes a steady Euler flow. An investigation of the influence of the boundary and the field topology on the relationship between the equilibrium flux function and the current density is described in §2.

In the magnetostatic context the formation of field discontinuities during relaxation has been invoked by Parker (1983, 1987) to explain the heating of the solar corona. Parker has argued that the slow motion of the footpoints of magnetic lines in the solar corona causes the magnetic field to readjust continuously to force-free states. This continuous relaxation of the field causes saddle points to collapse, creating current sheets which rapidly dissipate magnetic energy in their vicinity. In §3, we have found an infinite family of two-dimensional magnetostatic states describing the magnetic field in the vicinity of a collapsed saddle point. Each of these fields satisfies an equation similar to one analytically investigated by Parker (1990) and Vainshtein (1990).

2. Two dimensional magnetic relaxation of fields with the simplest topology

2.1. *Variational formulation*

Consider the magnetic relaxation of a field embedded in a two-dimensional domain $\mathscr{D}$, the magnetic field $\boldsymbol{B}$ being given by a flux function $\chi(x, y, t)$,

$$\boldsymbol{B} = (\partial\chi/\partial y, -\partial\chi/\partial x, 0). \tag{2.1}$$

The $\boldsymbol{B}$-lines are given by the contours $\chi(x, y, t) = \text{const.}$ and without loss of generality we can suppose that $\chi = 0$ on $\partial\mathscr{D}$. Suppose that the initial flux function $\chi_0(x, y)$ has only one stationary point $\mathscr{O}$ in the interior of $\mathscr{D}$ and that this is a maximum. Then $\boldsymbol{B} = 0$ at $\mathscr{O}$ and the $\boldsymbol{B}$-lines are elliptic in a neighbourhood of $\mathscr{O}$.

Let $\mathscr{A}(\chi_c)$ be the area enclosed by the contour line $\chi_0(x, y) = \chi_c$ where χ_c satisfies $0 \leqslant \chi_c \leqslant \chi_{\max}$. In this interval $\mathscr{A}(\chi_c)$ is monotonically decreasing with

$$\mathscr{A}(0) = \mathscr{A}_0 \quad \text{and} \quad \mathscr{A}(\chi_{\max}) = 0, \tag{2.2}$$

where $\mathscr{A}_0$ is the area of the domain $\mathscr{D}$. During relaxation the $\boldsymbol{B}$-lines are frozen in the fluid and the frozen field equation in two dimensions simplifies to $\mathrm{D}\chi/\mathrm{D}t = 0$. Since the flow is incompressible the area inside any such $\boldsymbol{B}$-line is conserved, which implies that the function $\mathscr{A}(\chi)$ continues to characterize the field for all times. It is thus reasonable to call $\mathscr{A}(\chi)$ the *signature function* of the field (Moffatt 1986).

The asymptotic equilibrium field described by a flux function $\chi^{\mathrm{E}}(x, y)$ satisfies

$$\nabla^2\chi^{\mathrm{E}} = F(\chi^{\mathrm{E}}) \tag{2.3}$$

for some current function $F(\chi^{\mathrm{E}})$, which will in principle be determined by the signature function and the shape of the boundary $\partial\mathscr{D}$.

The relationship between $F(\chi^{\mathrm{E}})$ and the signature function for a general boundary can be expressed via the following variational problem. The functional

$$M = \int_{\mathscr{D}} |\nabla\chi|^2 \,\mathrm{d}S \tag{2.4}$$

is to be minimized subject to the family of constraints

$$\int_{\chi(x,y)\geqslant\chi_{\mathrm{c}}} \mathrm{d}S = \mathscr{A}(\chi_{\mathrm{c}}). \tag{2.5}$$

Without the influence of the boundary, each $\boldsymbol{B}$-line would tend to minimize its length keeping its contained area constant; thus in the case of a circular or unbounded domain it is plausible to conclude that the whole field will relax to a configuration of concentric circles. For different boundary shapes however the boundary plays a constraining role and the general solution is non-trivial.

For any smooth field $\boldsymbol{G}(x,y)$, the two-dimensional divergence theorem states

$$\oint_{\chi(x,y)=\chi_{\mathrm{c}}} \boldsymbol{G}\cdot\boldsymbol{n}\,\mathrm{d}l = \int_{\chi(x,y)\geqslant\chi_{\mathrm{c}}} \nabla\cdot\boldsymbol{G}\,\mathrm{d}S. \tag{2.6}$$

Choosing $\boldsymbol{G} = (x,y)$ and using the fact that $\boldsymbol{n} = -\nabla\chi/|\nabla\chi|$, it follows that

$$\mathscr{A}(\chi_{\mathrm{c}}) = -\frac{1}{2}\oint_{\chi(x,y)=\chi_{\mathrm{c}}} \frac{x\chi_x + y\chi_y}{|\nabla\chi|}\,\mathrm{d}l. \tag{2.7}$$

Consider the area element $\delta\mathscr{A}$ contained between two smooth $\boldsymbol{B}$-lines with flux function values χ_{c} and $\chi_{\mathrm{c}}+\delta\chi_{\mathrm{c}}$. Then

$$\delta\mathscr{A} = \frac{\mathrm{d}\mathscr{A}(\chi_{\mathrm{c}})}{\mathrm{d}\chi_{\mathrm{c}}}\delta\chi_{\mathrm{c}} = \oint_{\chi(x,y)=\chi_{\mathrm{c}}} -\frac{\delta\chi_{\mathrm{c}}}{|\nabla\chi|}\,\mathrm{d}l$$

(cf. Batchelor 1955, §3) and therefore

$$\frac{\mathrm{d}\mathscr{A}(\chi_{\mathrm{c}})}{\mathrm{d}\chi_{\mathrm{c}}} = -\oint_{\chi(x,y)=\chi_{\mathrm{c}}} \frac{\mathrm{d}l}{|\nabla\chi|}. \tag{2.8}$$

Consider also the 'magnetic circulation' function

$$K(\chi_{\mathrm{c}}) = \oint_{\chi(x,y)=\chi_{\mathrm{c}}} \boldsymbol{B}\cdot\mathrm{d}\boldsymbol{x} = \oint_{\chi(x,y)=\chi_{\mathrm{c}}} |\nabla\chi|\,\mathrm{d}l. \tag{2.9}$$

By setting $\boldsymbol{G} = \nabla\chi$ in (2.6) we see that

$$K(\chi_{\mathrm{c}}) = -\int_{\chi(x,y)\geqslant\chi_{\mathrm{c}}} \nabla^2\chi\,\mathrm{d}S.$$

In equilibrium $\nabla^2\chi^{\mathrm{E}} = F(\chi^{\mathrm{E}})$ and thus

$$K(\chi_{\mathrm{c}}) = -\int_{\chi'=\chi_{\mathrm{c}}}^{\chi_{\max}} \oint_{\chi(x,y)=\chi'} \frac{F(\chi')}{|\nabla\chi|}\,\mathrm{d}l\,\mathrm{d}\chi' = \int_{\chi_{\mathrm{c}}}^{\chi_{\max}} F(\chi')\frac{\mathrm{d}\mathscr{A}}{\mathrm{d}\chi'}\,\mathrm{d}\chi'$$

or

$$F(\chi) = -\frac{\mathrm{d}K}{\mathrm{d}\chi}\Big/\frac{\mathrm{d}\mathscr{A}}{\mathrm{d}\chi}, \tag{2.10}$$

which is a result holding for all boundaries and signature functions. We thus see that the equilibrium current $-F(\chi^{\mathrm{E}}) = -\nabla^2\chi^{\mathrm{E}}$ is inversely proportional to $\mathrm{d}\mathscr{A}/\mathrm{d}\chi$ (which never vanishes) and is also proportional to the equilibrium rate of change of magnetic circulation across the $\boldsymbol{B}$-lines.

Returning to the variational form of this problem, the constraint equation (2.5) can be written as (2.7), or rather

$$\int_0^{\chi_{\max}} \frac{\mu(\chi)\,\mathscr{A}(\chi)}{\mathrm{d}\mathscr{A}/\mathrm{d}\chi}\,\mathrm{d}\chi = -\frac{1}{2}\int_0^{\chi_{\max}} \oint_{\chi(x,y)=\chi} \frac{\mu(\chi)\,(x\chi_x+y\chi_y)}{|\nabla\chi|\,\mathrm{d}\mathscr{A}/\mathrm{d}\chi}\,\mathrm{d}l\,\mathrm{d}\chi,$$

where $\mu(\chi)$ is the Lagrange multiplier function corresponding to the infinite number of constraints imposed by (2.5). The constraint equation (2.5) can be thus rewritten in the form

$$\int_{\mathscr{D}} \mu(\chi)\left[\frac{\mathscr{A}}{(\mathrm{d}\mathscr{A}/\mathrm{d}\chi)^2} - \frac{1}{2}\frac{x\chi_x+y\chi_y}{\mathrm{d}\mathscr{A}/\mathrm{d}\chi}\right]\mathrm{d}S = 0. \tag{2.11}$$

To minimize the energy functional (2.4) subject to the family of constraints (2.11) we construct the Lagrangian

$$\mathscr{L}(x,y,\chi,\chi_x,\chi_y) = \int_{\mathscr{D}} \left\{\chi_x^2+\chi_y^2+\mu(\chi)\left[\frac{\mathscr{A}}{(\mathrm{d}\mathscr{A}/\mathrm{d}\chi)^2} - \frac{1}{2}\frac{x\chi_x+y\chi_y}{(\mathrm{d}\mathscr{A}/\mathrm{d}\chi)}\right]\right\}\mathrm{d}S.$$

The Euler–Lagrange equation for stationary values of $\mathscr{L}$ is

$$\nabla^2\chi = \frac{\mu(\chi)}{\mathrm{d}\mathscr{A}/\mathrm{d}\chi}\frac{\mathrm{d}}{\mathrm{d}\chi}\left(\frac{\mathscr{A}}{\mathrm{d}\mathscr{A}/\mathrm{d}\chi}\right) + \frac{1}{2}\frac{\mathrm{d}\mu}{\mathrm{d}\chi}\frac{\mathscr{A}}{(\mathrm{d}\mathscr{A}/\mathrm{d}\chi)^2}. \tag{2.12}$$

We now define a new Lagrange multiplier function $\lambda(\chi)$ by

$$\lambda(\chi) = \mu(\chi) + \frac{\mathrm{d}\mathscr{A}/\mathrm{d}\chi}{2\mathscr{A}(\chi)}\int_{\chi}^{\chi_{\max}} \frac{\mathscr{A}(\chi')}{\mathrm{d}\mathscr{A}/\mathrm{d}\chi'}\frac{\mathrm{d}\mu}{\mathrm{d}\chi'}\,\mathrm{d}\chi'.$$

Hence $\lambda(\chi)$ and $\mu(\chi)$ are related through $\mathscr{A}(\chi)$ so that if $\lambda(\chi)$ is determined then $\mu(\chi)$ can be found also. The equation (2.12) is then equivalent to

$$\nabla^2\chi = \frac{\dfrac{\mathrm{d}}{\mathrm{d}\chi}\left(\lambda(\chi)\dfrac{\mathscr{A}}{\mathrm{d}\mathscr{A}/\mathrm{d}\chi}\right)}{\mathrm{d}\mathscr{A}/\mathrm{d}\chi}, \tag{2.13}$$

where the Lagrange multiplier function $\lambda(\chi)$ can be determined in principle by imposing the boundary condition (2.7). Comparing (2.13) to (2.10), it is evident that

$$\lambda(\chi) = -\frac{K(\chi)}{\mathscr{A}}\frac{\mathrm{d}\mathscr{A}}{\mathrm{d}\chi}. \tag{2.14}$$

2.2. *Dependence of the signature function on the boundary shape*

It was mentioned before that $\mathrm{d}\mathscr{A}/\mathrm{d}\chi < 0$, $\mathscr{A}(0) = \mathscr{A}_0$ and $\mathscr{A}(\chi_{\max}) = 0$. Are these all the restrictions on the signature function, and can $\mathrm{d}\mathscr{A}/\mathrm{d}\chi$ for example take any negative value throughout its domain? Consider a magnetic field inside a bounded convex domain $\mathscr{D}$ whose boundary contains a corner or cusp at a point $\mathscr{P}$; at this point the magnetic field $\boldsymbol{B}$ must vanish. Arbitrarily close to the boundary the $\boldsymbol{B}$-lines are smooth and thus $\mathrm{d}\mathscr{A}/\mathrm{d}\chi$ is given by (2.8). In the vicinity of $\mathscr{P}$, however, $|\boldsymbol{B}| = |\nabla\chi|$ can be chosen to be arbitrarily small which suggests that the integrand in (2.8)

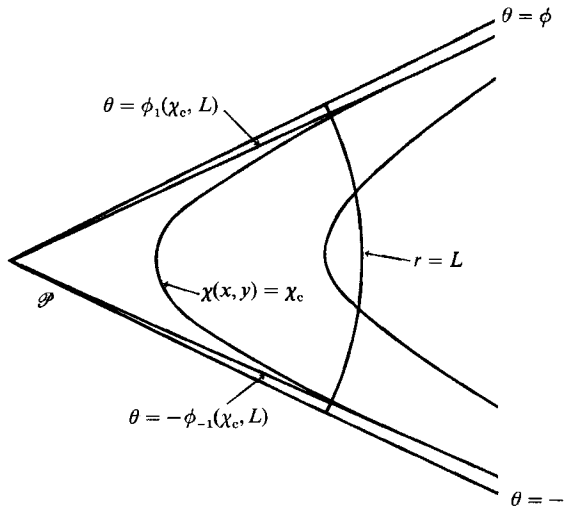

FIGURE 1. Form of a smooth field in the vicinity of a corner of angle $2\phi \leqslant \pi$.

must have an integrable singularity as $\chi \to 0$. (This is similar to the behaviour of the signature of Hill's spherical vortex (Moffatt 1988, §3).) To analyse the asymptotic behaviour of $\mathrm{d}\mathscr{A}/\mathrm{d}\chi$ close to a boundary containing a corner of angle 2ϕ assume that χ can be expanded in powers of r in a neighbourhood of the point $\mathscr{P}$. Let us assume that

$$\chi(r, \theta) = (r/a)^\alpha f(\theta) + \text{higher-order terms} \tag{2.15}$$

for $r \ll a$ and $-\phi \leqslant \theta \leqslant \phi$. Further assume that the current $-\nabla^2\chi$ is finite in the neighbourhood of $\mathscr{P}$, so that $\alpha \geqslant 2$. Since χ vanishes on $\partial\mathscr{D}$ this implies that

$$\left.\begin{aligned} f(\theta) &\sim a_1(\phi-\theta) + a_2(\phi-\theta)^2 + \ldots \quad \text{for} \quad \theta \sim \phi, \\ f(\theta) &\sim b_1(\phi+\theta) + b_2(\phi+\theta)^2 + \ldots \quad \text{for} \quad \theta \sim -\phi, \end{aligned}\right\} \tag{2.16}$$

the existence of fractional powers of $\phi \pm \theta$ smaller than two being excluded by assuming that the current is finite for $|\theta| < \phi$. Since the radial component of the magnetic field is also assumed to be non-vanishing on the boundary for $r \neq 0$, this implies that $a_1 \neq 0$ and $b_1 \neq 0$. Since the main contribution to the behaviour of $\mathrm{d}\mathscr{A}/\mathrm{d}\chi$ as $\chi \to 0$ comes from the neighbourhood of the point $\mathscr{P}$, the asymptotic behaviour can be calculated by integrating (2.8) along the $\boldsymbol{B}$-line $\chi(r, \theta) = \chi_c$ inside a radius $L \ll a$ from $\mathscr{P}$ (see figure 1):

$$\left(\frac{\mathrm{d}\mathscr{A}}{\mathrm{d}\chi}\right)_{\chi=\chi_c} \sim \chi_c^{-1+\frac{2}{\alpha}} \int_{-\phi_{-1}(\chi_c, L)}^{\phi_1(\chi_c, L)} \frac{\mathrm{d}\theta}{f(\theta)^{\frac{2}{\alpha}}} \quad \text{as} \quad \chi_c \to 0, \tag{2.17}$$

where $\chi_c = (L/a)^\alpha f(\sigma\phi_\sigma(\chi_c, L))$ for $\sigma = \pm 1$ and

$$\left.\begin{aligned} \chi_c &\sim (L/a)^\alpha a_1(\phi - \phi_1) \\ \chi_c &\sim (L/a)^\alpha b_1(\phi - \phi_{-1}) \end{aligned}\right\} \quad \text{as} \quad \chi_c \to 0,$$

and thus some elementary calculations give

$$\frac{\mathrm{d}\mathscr{A}}{\mathrm{d}\chi} \sim \left\{\begin{aligned} &\log\chi \quad \text{for} \quad \alpha = 2 \\ &\chi^{-1+\frac{2}{\alpha}} \quad \text{for} \quad \alpha > 2 \end{aligned}\right\} \quad \text{as} \quad \chi \to 0. \tag{2.18}$$

2.3. *Dependence of the equilibrium magnetic circulation on the boundary shape*

We similarly expect that any possible singular behaviour of $\mathrm{d}K(\chi_c)/\mathrm{d}\chi_c$ as $\chi_c \to 0$ will be caused by the existence of corners or cusps on the boundary. In the case of a non-re-entrant corner (subtending an angle smaller than π radians) assume again that near $\mathscr{P}$, χ satisfies (2.15), (2.16). Then by similarly integrating (2.9) along a $\boldsymbol{B}$-line $\chi(x,y) = \chi_c$ inside a radius L from $\mathscr{P}$ and by letting $\chi_c \to 0$

$$K(\chi_c) \sim \chi_c \int_{-\phi_{-1}(\chi_c, L)}^{\phi_1(\chi_c, L)} \left[\frac{f'(\theta)}{f(\theta)}\right]^2 \mathrm{d}\theta + \kappa\chi_c, \tag{2.19}$$

where κ is a non-zero constant. The main contribution to this integral comes from the points where $f(\theta)$ is small, i.e. from the endpoints of integration. Substituting $f(\theta)$ from (2.16), one finds that

$$\frac{\mathrm{d}K(\chi)}{\mathrm{d}\chi} \sim \begin{cases} \log\chi & \text{when} \quad a_2^2 + b_2^2 \neq 0 \\ \kappa & \text{when} \quad a_2^2 + b_2^2 = 0 \end{cases} \quad \text{as} \quad \chi \to 0. \tag{2.20}$$

It thus transpires that the asymptotic form of $\mathrm{d}\mathscr{A}/\mathrm{d}\chi$ as $\chi \to 0$ only depends on the r-scaling of the magnetic field in the vicinity of the corner while $\mathrm{d}K/\mathrm{d}\chi$ only depends on the angular variations of χ. If the boundary contains more than one corner then the field inside the corner which gives the dominant contribution to the signature function will have to preserve its r-scaling for the signature function to be conserved.

Suppose the equilibrium field behaves like

$$\chi^{\mathrm{E}}(r,\theta) = (r/a)^{\alpha} f^{\mathrm{E}}(\theta) + \text{higher-order terms}$$

with
$$f^{\mathrm{E}}(\theta) \sim a_1^{\mathrm{E}}(\phi - \theta) + a_2^{\mathrm{E}}(\phi - \theta)^2 + \ldots \quad \text{for} \quad \theta \sim \phi,$$
$$f^{\mathrm{E}}(\theta) \sim b_1^{\mathrm{E}}(\phi + \theta) + b_2^{\mathrm{E}}(\phi + \theta)^2 + \ldots \quad \text{for} \quad \theta \sim -\phi.$$

The Grad–Shafranov equation (2.3) indicates that the equilibrium current must have the same value on each $\boldsymbol{B}$-line. If $\alpha > 2$ then $j_z = -r^{\alpha-2}[f^{\mathrm{E}''}(\theta) + \alpha^2 f^{\mathrm{E}}(\theta)]$ to the lowest order in r, and by taking the limit $r \to 0$ it is obvious that the equilibrium volume current density must vanish as we approach $\partial\mathscr{D}$. (Note that a current sheet $\boldsymbol{j}_s = -\boldsymbol{n} \wedge \boldsymbol{B}|_{\partial\mathscr{D}}$ may flow on the boundary.) This immediately implies that $a_2^{\mathrm{E}} = b_2^{\mathrm{E}} = 0$ unless $\alpha = 2$. Combining (2.10), (2.18) and (2.20), it can be concluded that the asymptotic forms of the equilibrium current as $\chi \to 0$ due to a corner on the boundary are

$$\nabla^2\chi \sim \begin{cases} \chi^{1-\frac{2}{\alpha}} & \text{for} \quad \alpha > 2 \\ 1/\log\chi & \text{for} \quad \alpha = 2 \quad \text{and} \quad a_2^{\mathrm{E}} = b_2^{\mathrm{E}} = 0 \\ \text{constant} & \text{for} \quad \alpha = 2 \quad \text{and} \quad (a_2^{\mathrm{E}})^2 + (b_2^{\mathrm{E}})^2 \neq 0. \end{cases} \tag{2.21}$$

Therefore the equilibrium volume current always tends to zero as we approach the boundary unless $\alpha = 2$ and $a_2^{\mathrm{E}} = b_2^{\mathrm{E}} = 0$ whence it can take a finite non-zero value.

2.4. *Properties of* $\lambda(\chi)$

As mentioned above, $\lambda(\chi)$ can be either thought of as a Lagrange multiplier for a variational problem or defined through $K(\chi) = -\lambda(\chi)\mathscr{A}/(\mathrm{d}\mathscr{A}/\mathrm{d}\chi)$. Hence, from (2.14)

$$\lambda(\chi_c) = \frac{1}{\mathscr{A}(\chi_c)} \oint_{\chi(x,y)=\chi_c} \frac{\mathrm{d}l}{|\nabla\chi|} \oint_{\chi(x,y)=\chi_c} |\nabla\chi|\,\mathrm{d}l \tag{2.22}$$

and by using the Cauchy–Schwarz inequality it can be shown that

$$\lambda(\chi) \geqslant \mathscr{L}^2(\chi)/\mathscr{A}(\chi), \tag{2.23}$$

where $\mathscr{L}(\chi_c)$ is the length of the $\boldsymbol{B}$-line $\chi(x,y)=\chi_c$ and $\mathscr{A}(\chi_c)$ is the area it contains. Thus λ is always larger than 4π and the equality in relation (2.23) is attained only when $|\nabla\chi|$ is constant along the $\boldsymbol{B}$-line.

A set of $\boldsymbol{B}$-lines $\chi(x,y)=$ const. is self-similar with respect to an elliptic point at the origin when $\chi(\alpha x,\alpha y)-\chi_{\max}=h(\alpha)\,(\chi(x,y)-\chi_{\max})$ with $h(1)=1$. This means that any uniformly stretched $\boldsymbol{B}$-line $(x,y)\to\alpha(x,y)$ coincides with another $\boldsymbol{B}$-line of the set.

LEMMA. *If* $x\chi_x+y\chi_y=F(\chi)$ *then* $\chi(x,y)$ *describes a set of self-similar* $\boldsymbol{B}$*-lines.*

Proof. If f is a monotonic function and $\chi(x,y)$ describes a set of $\boldsymbol{B}$-lines then $f(\chi(x,y))$ also describes the same set since $\chi(x,y)=$ const. implies that $f(\chi(x,y))=$ const. Given that $x\chi_x+y\chi_y=F(\chi)$ we seek a function $\phi(x,y)=f(\chi(x,y))$ such that

$$x\phi_x+y\phi_y=c(\phi-\phi_{\max}) \tag{2.24}$$

with $\phi_{\max}=f(\chi_{\max})$ and hence

$$F(\chi)\,\mathrm{d}f/\mathrm{d}\chi=c[f(\chi)-f(\chi_{\max})] \tag{2.25}$$

which has a solution if $F(\chi)$ only vanishes at $\chi=\chi_{\max}$ (since f is assumed to be monotonic). Considering the general solution of (2.24)

$$\phi(x,y)=\phi_{\max}+\int a(\lambda)\,x^{\lambda}y^{c-\lambda}\,\mathrm{d}\lambda$$

it is obvious that $\phi(x,y)-\phi_{\max}$ is a homogeneous function of order c, therefore

$$\phi(\alpha x,\alpha y)-\phi_{\max}=\alpha^c(\phi(x,y)-\phi_{\max}).$$

Thus if ϕ describes a set of self-similar $\boldsymbol{B}$-lines, then so does χ. □

Example. The flux function $\chi=\chi_{\max}\sin(\frac{1}{2}\pi-x^2-y^2)$ satisfies

$$x\chi_x+y\chi_y=-2\chi_{\max}(\tfrac{1}{2}\pi-\arcsin(\chi/\chi_{\max}))\,[1-(\chi/\chi_{\max})^2]^{\frac{1}{2}}=F(\chi).$$

Equation (2.25) then gives that $\phi(x,y)=f(\chi(x,y))$ with

$$f(\chi)=f(\chi_{\max})-\tfrac{1}{2}\pi+\arcsin(\chi/\chi_{\max})$$

satisfies $x\phi_x+y\phi_y=2\phi$ which proves that both ϕ and χ are self-similar flux functions.

If the equilibrium field resulting from a relaxation procedure has self-similar $\boldsymbol{B}$-lines then the constraint equation (2.7) can be simply written as $\mathscr{A}=\frac{1}{2}(x\chi_x+y\chi_y)\,\mathrm{d}\mathscr{A}/\mathrm{d}\chi$. This simplified form leads to (2.13) with $\lambda(\chi)=$ const. Consider now two flux functions $\chi_1(x,y)$ and $\chi_2(x,y)=f(\chi_1(x,y))$ with $f(\chi)$ being a monotonic function such that both flux functions vanish on the boundary and attain the same maximum value $\chi_{\max}$ at the elliptic point. The $\boldsymbol{B}$-lines of the two fields are geometrically identical although the magnetic field might not take the same value at geometrically equivalent points. Let us consider the values of λ corresponding to two geometrically identical $\boldsymbol{B}$-lines of the two fields, say $\chi_1(x,y)=\chi_c$ and $\chi_2(x,y)=f(\chi_c)$. Then using (2.22)

$$\left.\begin{aligned}\lambda_1(\chi_c)&=\frac{1}{\mathscr{A}_1(\chi_c)}\oint_{\chi_1(x,y)=\chi_c}\frac{\mathrm{d}l}{|\nabla\chi_1|}\oint_{\chi_1(x,y)=\chi_c}|\nabla\chi_1|\,\mathrm{d}l\\ \lambda_2(f(\chi_c))&=\frac{1}{\mathscr{A}_2(f(\chi_c))}\oint_{f(\chi_1)=f(\chi_c)}\frac{\mathrm{d}l}{\dfrac{\mathrm{d}f(\chi_c)}{\mathrm{d}\chi_c}|\nabla\chi_1|}\oint_{f(\chi_1)=f(\chi_c)}\frac{\mathrm{d}f(\chi_c)}{\mathrm{d}\chi_c}|\nabla\chi_1|\,\mathrm{d}l.\end{aligned}\right\} \tag{2.26}$$

Since f is a monotonic function, $f(\chi_1) = f(\chi_c)$ implies that $\chi_1(x,y) = \chi_c$ and $\mathscr{A}_2(f(\chi_c)) = \mathscr{A}_1(\chi_c)$ since the two flux lines considered are geometrically identical. Therefore $\lambda_1(\chi_c) = \lambda_2(f(\chi_c))$ which proves that $\lambda(\chi)$ is a purely geometrical property of the $\boldsymbol{B}$-lines. This also explains why $\lambda(\chi)$ is constant when the $\boldsymbol{B}$-lines are self-similar, since they all have the same shape.

The dependence of the current distribution on the boundary shape is maintained through $\lambda(\chi)$ since the boundary is a $\boldsymbol{B}$-line and thus $\lambda(\chi)$ implicitly depends on its shape. For example, for $\chi = 1-(x/a)^{2n}-(y/b)^{2n}$ a simple calculation yields

$$\lambda(n) = 4\left(\frac{a}{b}+\frac{b}{a}\right)\left(\frac{1}{n}-\frac{1}{2n^2}\right)\frac{\pi}{\sin(\pi/2n)}.$$

For $n = 1$, $\lambda = 2\pi(a/b+b/a)$ (result for circles and ellipses) and for $n\to\infty$, $\lambda\to 16$ although such a field would be unphysical because it represents a set of self-similar square-shaped $\boldsymbol{B}$-lines with discontinuous magnetic field at the vertices. However for n finite $|\lambda(n)| < 16$. Hence λ attains its infimum (4π) in the case of concentric circles.

Consider a magnetic field $\boldsymbol{B}_0(\boldsymbol{x})$ with the usual elliptic topology extending to infinity. Let $\chi(x,y) = \chi_{\max}$ at the origin and $\chi\to 0$ as $r\to\infty$. Assume further that the field's strength falls off faster than $1/r$ so that the total magnetic energy $M(0)$ is finite. If the field is left to relax magnetically then in equilibrium the final energy M^{E} will be given by

$$2M^{\mathrm{E}} = \int|\nabla\chi|^2\,\mathrm{d}S = \int_{\chi=0}\chi\nabla\chi\cdot\boldsymbol{n}\,\mathrm{d}l-\int_{\mathscr{D}}\chi\nabla^2\chi\,\mathrm{d}S = \int_{\chi_{\max}}^{0}\chi\frac{\mathrm{d}K}{\mathrm{d}\chi}\mathrm{d}\chi. \tag{2.27}$$

A simple integration by parts using (2.27) then gives

$$M^{\mathrm{E}} = -\frac{1}{2}\int_0^{\chi_{\max}}\lambda(\chi)\frac{\mathscr{A}}{\mathrm{d}\mathscr{A}/\mathrm{d}\chi}\mathrm{d}\chi. \tag{2.28}$$

Therefore, since $\mathscr{A}(\chi)$ is invariant, the minimum energy of the field is attained when λ is minimized. Since in this case there is no boundary constraining the behaviour of $\lambda(\chi)$, the minimum energy is attained when $\lambda(\chi) = 4\pi$ and all the $\boldsymbol{B}$-lines have relaxed to circles. This argument shows that this configuration has the least possible energy but to show that such a state is topologically accessible one must find a continuous incompressible flow that can advect the initial field to the final one. From the theory of suspensions in dynamical systems (Arrowsmith & Place 1990, p. 36) it is known that if a continuous area-preserving orientable map can be found such that it maps the initial field to the final configuration we are interested in, then the required flow can be constructed from this map. (This theorem is valid under certain restrictive conditions which are certainly satisfied for the maps from $\mathbb{R}^2$ to $\mathbb{R}^2$ with which we are concerned here.) It is therefore required to map an initial field $\boldsymbol{B}_0$ to a final field $\boldsymbol{B}^{\mathrm{E}}$ with circular lines of force which represents the minimum energy state. Thus every initial point $(r,\theta)\to(r',\theta')$, where $\pi r'^2 = \mathscr{A}(\chi(r,\theta))$ since the area inside every $\boldsymbol{B}$-line is conserved, and $\theta'(r,\theta)$ is unknown. For the map to be area-preserving and orientable

$$\frac{r'}{r}\left(\frac{\partial r'}{\partial r}\frac{\partial\theta'}{\partial\theta}-\frac{\partial r'}{\partial\theta}\frac{\partial\theta'}{\partial r}\right) = 1.$$

This equation's characteristics are the initial $\boldsymbol{B}$-lines, hence a solution for θ' in the whole plane exists excluding the origin. A local analysis of the solution's behaviour in the vicinity of the origin shows that we can analytically continue the solution for

θ' there. Naturally some 'initial' condition must be imposed on θ'; an example is $\theta'(r,0)=0$. We have thus shown that the ground-state energy configuration for a magnetic field with an elliptic topology extending to infinity is one in which all the $\boldsymbol{B}$-lines have relaxed to circles.

To conclude this section it should be noted that $\lambda(\chi_c)$ depends on the shape of the $\boldsymbol{B}$-line $\chi(x,y)=\chi_c$ and also on the way this shape is changing with χ_c. This is indicated by its behaviour when the boundary has a corner or a cusp at a point $\mathscr{P}$ say. In such a case $\mathrm{d}\mathscr{A}/\mathrm{d}\chi\to-\infty$ as $\chi\to 0$ but $K(\chi)$ remains bounded everywhere, which implies that $\lambda\to\infty$ there. This singular behaviour indicates the difficulty of approaching a non-smooth boundary with smooth $\boldsymbol{B}$-lines. Another way of interpreting this behaviour is to think of the Lagrange multiplier function as some sort of weighting for the infinite number of constraints described by (2.7). The fact that λ becomes infinite on any boundary containing a sharp point indicates the strong constraint imposed by such a corner or cusp.

2.5. *Numerical results*

All the numerical experiments presented here were performed inside a square of unit area. A magnetostatic equilibrium solution inside a square is given by $\xi=\sin\pi x\sin\pi y$, and three initial fields of the form $\chi_0=f(\xi)$ have been considered. By varying f three different appropriate signature functions were chosen and then the system was allowed to relax numerically using the dynamical prescription described in §1 governed by the energy evolution equation (1.7). This model leads to a system of two coupled partial differential equations of the form

$$\frac{\partial\chi}{\partial t}=\frac{\partial(\psi,\chi)}{\partial(x,y)},\qquad \nabla^2\psi=-\frac{\partial(\chi,\nabla^2\chi)}{\partial(x,y)}, \tag{2.29}$$

where $\boldsymbol{B}=\nabla\wedge(0,0,\chi)$ and $\boldsymbol{u}=\nabla\wedge(0,0,\psi)$. These equations were discretized and then solved on a uniform mesh of size 65^2. To discretize (2.29) one must bear in mind that we must calculate up to third-order derivatives of the function χ. To limit errors to order h^2 in such derivatives we must calculate the first-order derivatives to order-h^3 accuracy where h is the mesh size. Minimizing the error in the first-derivative estimate of any smooth function f (Iserles & Nørsett 1991, p. 124) one gets

$$f'(x_0)=\sum_{j=-r}^{s}\frac{\beta_j f_j}{h}+O(h^{r+s}),$$

where $r+s+1$ is the number of grid points we use, $f_l=f(x_0+lh)$ and the coefficients β_j are given by

$$\beta_j=\frac{(-1)^{j+1}}{j}\frac{r!\,s!}{(r+j)!\,(s-j)!},\quad j=-r,\ldots,s,\quad j\neq 0$$

and

$$\beta_0=\begin{cases}-\displaystyle\sum_{i=r+1}^{s}\frac{1}{i} & :\quad s\leqslant r+1\\ 0 & :\quad s=r\\ \displaystyle\sum_{i=s+1}^{r}\frac{1}{i} & :\quad r\leqslant s+1.\end{cases}$$

It is very easy to generalize these formulae for functions of two variables and I have chosen $r+s=4$ at all points on the grid, e.g. $r=0$, $s=4$ or $r=4$ and $s=0$ on the

boundary. Two methods were used to solve the Poisson equation; the multigrid method and a fast Poisson solver. The latter proved to be much more efficient and all the results shown here were produced using the IMSL library solver. The time-stepping methods experimented with were the Euler method, the fourth-order Runge–Kutta method with variable step size and the Burlisch–Stoer method. For a small number of points on the grid the Burlisch–Stoer routine was the fastest and most accurate, but for more refined meshes the fourth-order Runge–Kutta method proved to be more robust and significantly faster.

The first field considered is

$$\chi_0 = (e^{5\xi} - 1)/W, \tag{2.30}$$

with W being a normalizing factor so that $|\chi_0|_{\max} = 1$. As figure 2(*a*) shows this represents a magnetic field which is strong in the centre of the square. By comparing the relaxed field χ^E in figure 2(*b*) to the initial field it can be seen that the $\boldsymbol{B}$-lines have become more circular, confirming the anticipated tendency of $\boldsymbol{B}$-lines to minimize their length while conserving the area they enclose. The plot of $\nabla^2\chi_0$ against χ_0 in figure 2(*c*) is as expected a scatter of points since the field is not in magnetostatic equilibrium although since the scatter is quite limited the field is perhaps not far from it. Since $\chi_0 \sim xy$ in the vicinity of each corner the field is in equilibrium there up to the first order in r. We therefore expect that $\nabla^2\chi^E = 0$ at $\chi^E = 0$. This is confirmed in the dotted plot of $\nabla^2\chi^E$ against χ^E in figure 2(*d*). The Grad–Shafranov equation predicts a functional relationship between $\nabla^2\chi^E$ and χ^E, as seen in this figure.

The local Taylor expansion of χ^E near the elliptic point at (0,0) has the form $\chi^E = \chi_{\max} - c_1 x^2 - c_2 y^2 + \ldots$, where $c_1 = c_2$ by symmetry. Hence sufficiently close to the centre the $\boldsymbol{B}$-lines are circles so that $\lambda(\chi_{\max}) = 4\pi$. The solid line in figure 2(*d*) is the value of $F(\chi^E)$ predicted from (2.13) assuming that $\lambda(\chi) = 4\pi$ for all values of χ. This is of course a crude approximation since we know that $\lambda(\chi) \to \infty$ for $\chi \to 0$. Still the agreement between the dotted and solid curves was so good that one of them had to be slightly shifted to render them distinguishable. Figure 2(*e*) shows the magnetic energy during relaxation which by (1.7) decreases monotonically with time. In all computations the total magnetic energy was calculated at each time step and the program automatically stopped as soon as the energy started increasing due to numerical instabilities. Finally figure 2(*f*) shows the signature function of the initial field (solid line) which should be conserved during relaxation. Since the analytic form of the final field is unknown the only way to estimate the final field's signature function is to count the number of mesh points inside every $\boldsymbol{B}$-line. This method can only provide us with a very rough estimate of the signature function and the laddered appearance of such plots (dotted line in the same figure) is pronounced at points where the mesh is not fine enough for such an estimate to be accurate. The reasonable agreement of the dotted and solid curves does nevertheless confirm that the signature function is conserved to a good approximation.

The next field considered is

$$\chi_0 = (e^{-5\xi} - 1)/W, \tag{2.31}$$

with W being the usual normalizing factor. This magnetic field shown in figure 3(*a*) is strong close to the boundary of the domain. The relaxed field χ^E in figure 3(*b*) is interesting since the $\boldsymbol{B}$-lines in this case have become less circular as time evolved. To understand this behaviour consider the problem of an isolated flux tube inside the unit square. If the area it encloses is smaller than $\frac{1}{4}\pi$ then the tube can become circular and thus will tend to do so during relaxation. When the area it encloses is larger than $\frac{1}{4}\pi$ the flux tube cannot become circular since it would not then fit inside

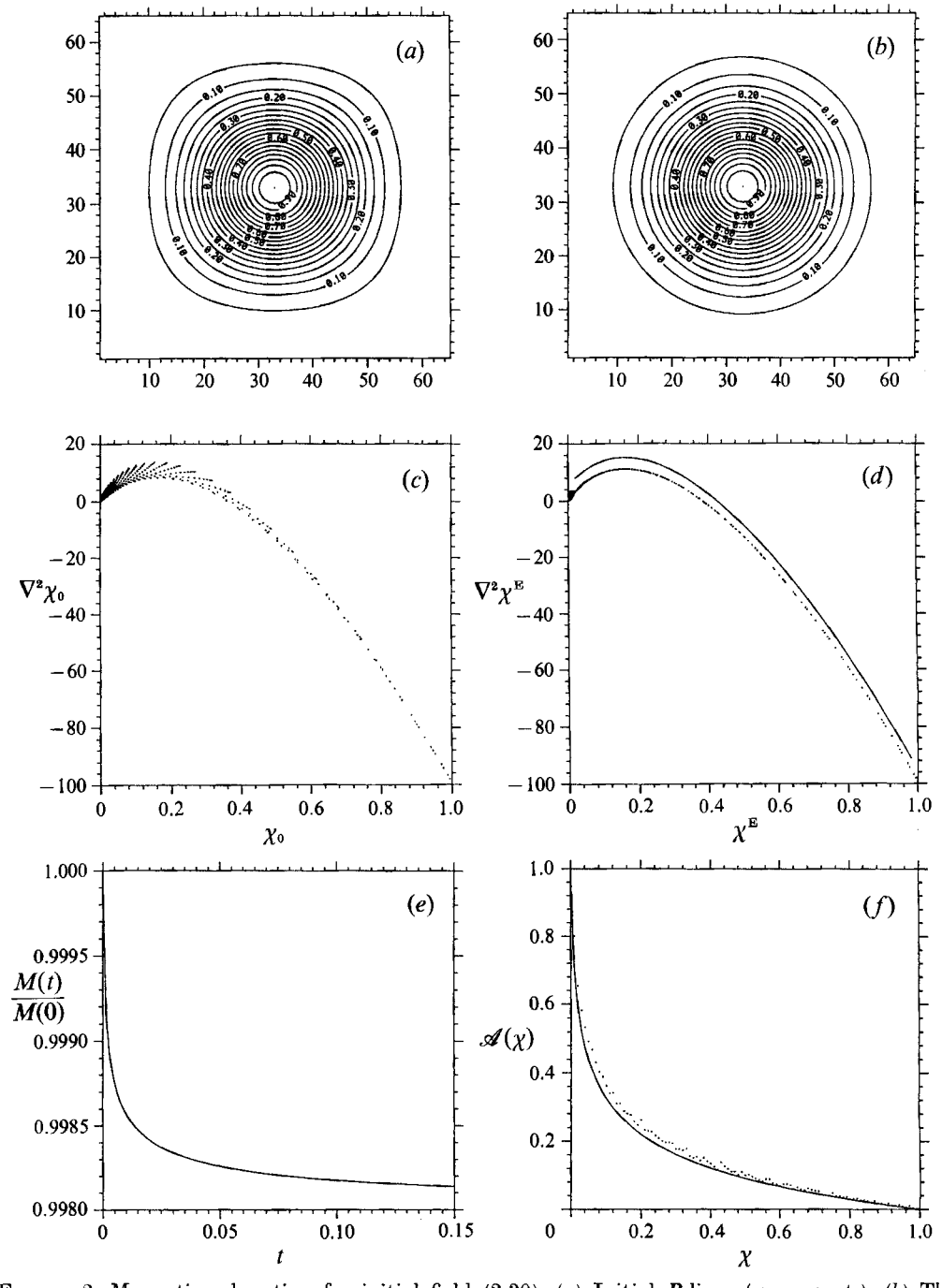

FIGURE 2. Magnetic relaxation for initial field (2.30). (*a*) Initial $\boldsymbol{B}$-lines ($\chi_0 = \text{const.}$). (*b*) The numerically relaxed field χ^E. (*c*) $\nabla^2\chi_0$ against χ_0. This is just a scatter of points since χ_0 is not in equilibrium. (*d*) $\nabla^2\chi^E$ against χ^E (dotted line) giving evidence of a functional relationship between the equilibrium current $-\nabla^2\chi^E$ and the equilibrium flux function χ^E. The solid line shows the predicted functional relationship using (2.13) and assuming that $\lambda(\chi) = 4\pi$. (*e*) Magnetic energy during relaxation of the field (the initial energy has been normalized to unity). (*f*) Signature function for the initial field (solid line) and final field (dotted line obtained by counting mesh points inside $\boldsymbol{B}$-lines).

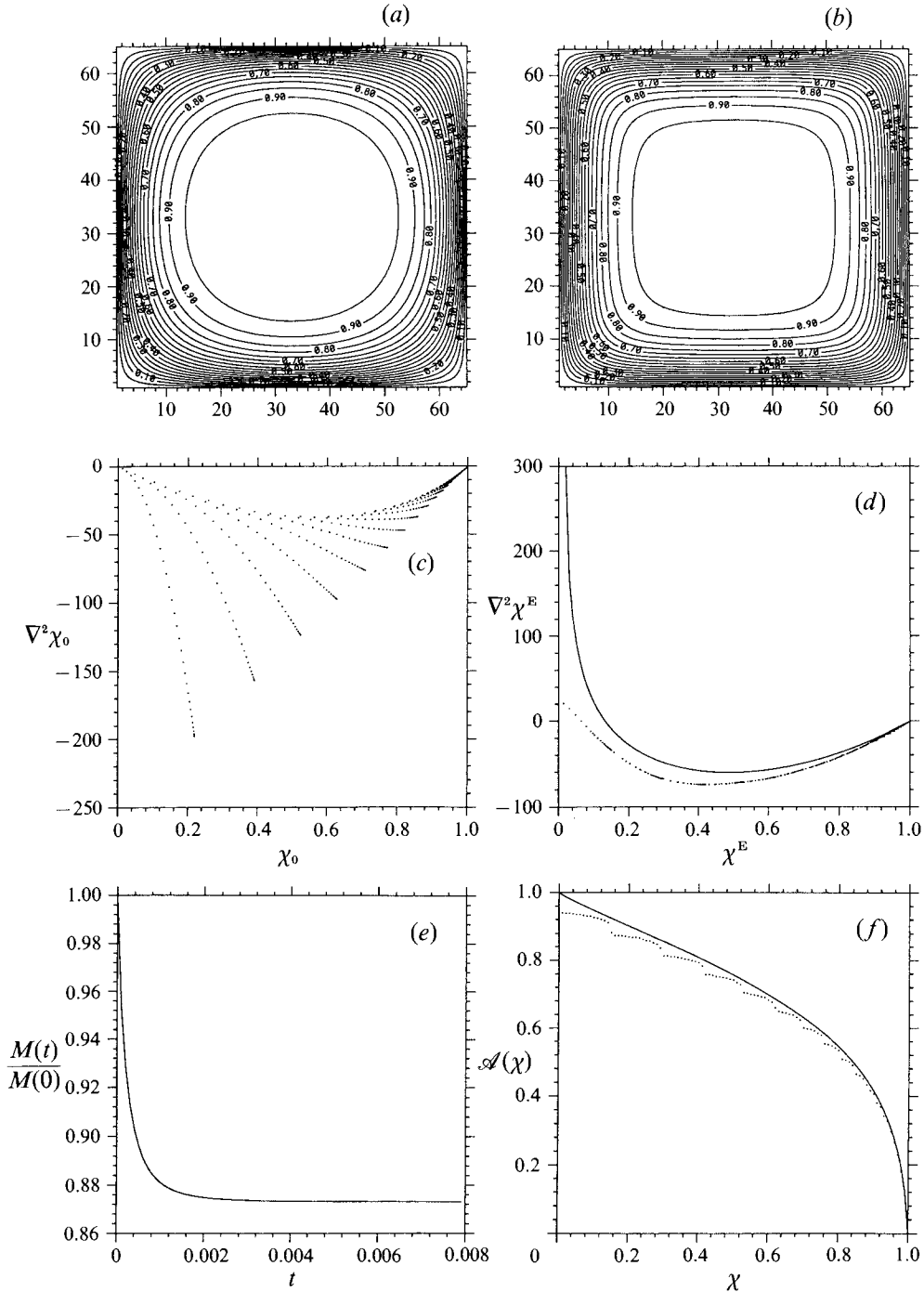

FIGURE 3. Magnetic relaxation results for field (2.31). (*a*)–(*f*) See caption for figure 2. Here the $\boldsymbol{B}$-lines become less circular since most of the field is concentrated close to the boundary. The approximation $\lambda(\chi) \approx 4\pi$ is therefore less accurate in predicting the current function $F(\chi^E)$.

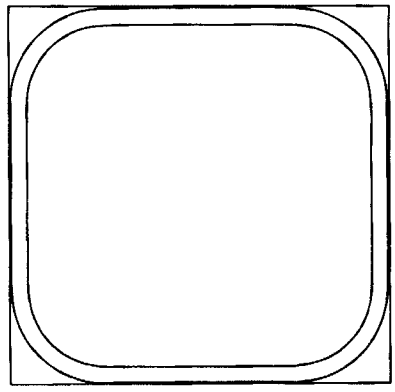

FIGURE 4. Minimum energy state for an isolated flux tube confined inside a square of unit area and enclosing an area larger than $\frac{1}{4}\pi$.

the square. The boundary imposes an extra constraint on the tube which forces it to touch the sides of the square and join the straight segments with arcs of circles which are tangential to them at the points of contact (figure 4). In the same way the global problem of minimizing the energy of a general field gives rise to two opposing tendencies. The field lines which would fit in the boundary if they became circular try to do so while those which would not tend to follow the boundary shape. When the field energy is concentrated near the boundary, this boundary effect is dominant and the field evolves in this counterintuitive fashion. Figure 3(*c*) is the plot of $\nabla^2\chi_0$ against χ_0 and in comparison to figure 2(*c*) the scatter of points here is much more pronounced. The asymptotic behaviour of χ_0 close to the corners is as before so that again we expect $\nabla^2\chi^{\mathrm{E}} = 0$ at $\chi^{\mathrm{E}} = 0$. The dotted plot of $\nabla^2\chi^{\mathrm{E}}$ against χ^{E} in figure 3(*d*) does not indicate this, although it confirms a clear functional relationship between the current and flux function of the magnetostatic field. The behaviour near $\chi^{\mathrm{E}} = 0$ is, no doubt, due to the fact that the function $F(\chi^{\mathrm{E}})$ has a steep gradient in the neighbourhood of $\chi^{\mathrm{E}} = 0$ and thus cannot be resolved with such a rough mesh (65^2). The predicted current assuming that $\lambda(\chi) = 4\pi$ is shown by the solid line in figure 3(*d*) and is now clearly quite inaccurate. The reason is that by assuming that $\lambda(\chi) = 4\pi$ for every χ we have not taken account of the effect of a non-circular boundary. Since the field is strong close to the boundary it is not surprising that this approximation will be less accurate. It should be noted though that the qualitative behaviour of $F(\chi^{\mathrm{E}})$ is still captured. Figure 3(*e*) shows the magnetic energy during relaxation, the equilibrium energy being reached very rapidly. The solid line in figure 3(*f*) is the initial field's signature function while the dotted one is the equilibrium field's estimate of the signature function.

The last field considered is

$$\chi = \{\sinh(10) + \sinh[20(\xi - \tfrac{1}{2})]\}/W, \tag{2.32}$$

providing a magnetic field that is strong both close to the centre and close to the boundary of the square (figure 5*a*). The equilibrium field in figure 5(*b*) χ^{E} shows that the two parts of the field evolve as if they were decoupled: the central $\boldsymbol{B}$-lines become more circular and those close to the boundary become more nearly square. The plot of $\nabla^2\chi_0$ against χ_0 in figure 5(*c*) is more scattered for small values of χ_0, i.e. close to the boundary. The field has the same asymptotic form in the corners as in the previous examples and the dotted plot of $\nabla^2\chi^{\mathrm{E}}$ against χ^{E} in figure 5(*d*) does suggest that the equilibrium current vanishes on the boundary. The $F(\chi^{\mathrm{E}})$ prediction when

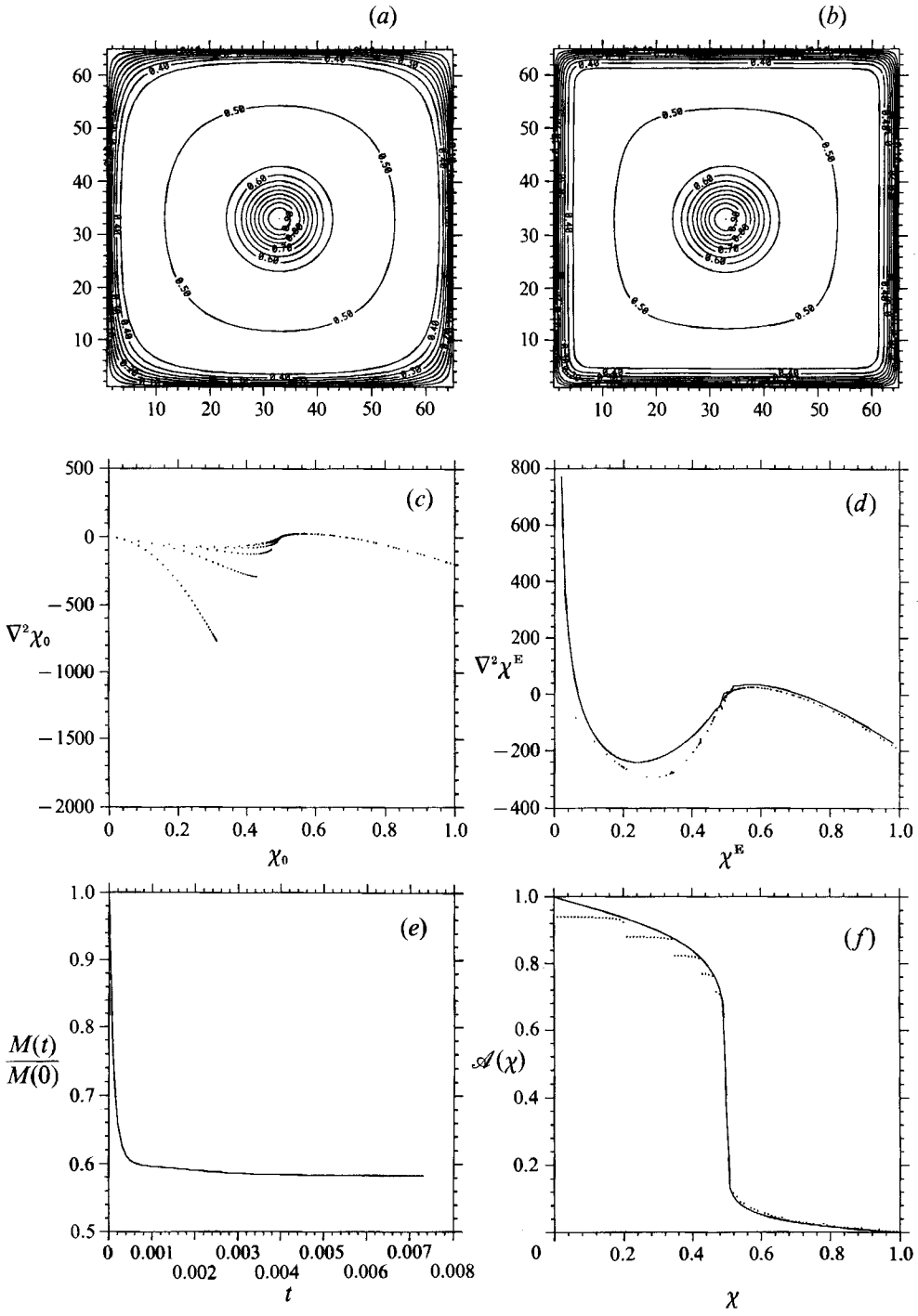

FIGURE 5. Magnetic relaxation results for field (2.32). (*a*)–(*f*) See caption for figure 2. Here the strong $\boldsymbol{B}$-line in the centre and near the boundary act as if they are decoupled; hence the former become more circular and the latter less. As before the current prediction is less accurate close to the boundary.

it is assumed that $\lambda(\chi) = 4\pi$ is again shown by the solid line in this figure. This prediction had to be slightly shifted since it perfectly overlapped with the numerical result for $\chi > 0.5$, although for small values of χ the agreement was not perfect. The field's energy during relaxation (figure 5*e*) shows rapid relaxation associated with the central field followed by much slower relaxation associated with the boundary field. The solid line in figure 5(*f*) is the initial field's signature function with the dotted one being the equilibrium field's estimate of the signature function.

It is interesting that in all three cases considered the scatter of points in the plots of the initial current against the initial flux function values was more pronounced for small values of χ_0, i.e. close to the boundary. This suggests that the magnetic fields evolve so as to accommodate as well as possible the strong constraints imposed on them by the boundary.

3. Two-dimensional magnetic relaxation of fields with saddle points

3.1. *Equilibrium field in the vicinity of a* Y*-point*

Consider now a field $\chi_0(x, y)$ containing one or more saddle points which is allowed to relax. Since the $\boldsymbol{B}$-lines are hyperbolic in the neighbourhood of each saddle point, the Lorentz force may cause the angle between the separatrices to collapse to zero and tangential discontinuities of $\boldsymbol{B}$ may form through this mechanism. In general any initial field $\chi_0(x, y)$ will be topologically characterized by the topology of the web of separatrices that divide the domain $\mathscr{D}$ into n subdomains and by the n signature functions corresponding to these subdomains.

The fields considered here divide the flow domain into three or four subdomains $\mathscr{D}_i$ with corresponding signature functions $\mathscr{A}_i(\chi)$. The domain used is the unit square and χ_0 vanishes on the separatrices. As a generalization of (2.13) the equilibrium field χ^{E} is expected to satisfy

$$\nabla^2\chi^{\mathrm{E}} = \frac{\dfrac{\mathrm{d}}{\mathrm{d}\chi^{\mathrm{E}}}\left(\lambda_i(\chi^{\mathrm{E}})\dfrac{\mathscr{A}_i}{\mathrm{d}\mathscr{A}_i/\mathrm{d}\chi^{\mathrm{E}}}\right)}{\mathrm{d}\mathscr{A}_i/\mathrm{d}\chi^{\mathrm{E}}} \quad \text{in} \quad \mathscr{D}_i \quad \text{for} \quad i = 1, 2, \ldots. \tag{3.1}$$

This equation has to be solved subject to the constraint that the total pressure is continuous on $\partial\mathscr{D}_i$ for $i = 1, 2, \ldots$. An additional complication comes from the fact that in (2.13) $\lambda(\chi)$ depended implicitly on the boundary shape, which was fixed. Now, each $\lambda_i(\chi)$ depends on the boundary shape of the subdomain $\mathscr{D}_i$ which is not fixed. The analysis of the behaviour of the signature function in the presence of a corner on the boundary is also valid for a corner formed by the separatrices and it is thus interesting to investigate whether an initial field that in the vicinity of the saddle point behaves like

$$\chi_0(r, \theta) = (r/a)^{\alpha} f_0(\theta) + \text{higher-order terms}$$

can give relaxed solutions obeying (2.21) and describing a collapsed saddle point.

We assume that the saddle point has collapsed onto a current sheet on the line $\theta = \pi$ and that the three separatrices forming the Y-point divide the domain $\mathscr{D}$ into the three convex subdomains

$$\begin{aligned}
&\mathscr{D}_1\colon \quad -\theta_1 \leqslant \theta \leqslant \theta_2 \quad (\theta_1 \geqslant 0, \theta_2 \geqslant 0),\\
&\mathscr{D}_2\colon \quad \theta_2 \leqslant \theta \leqslant \pi,\\
&\mathscr{D}_3\colon \quad -\pi \leqslant \theta \leqslant -\theta_1.
\end{aligned}$$

Equations (2.21) are modified by replacing the term $\chi^{1-2/\alpha}$ by $|\chi|^{1-2/\alpha}$. This is necessary since χ can now be both negative and positive in the vicinity of the saddle point. We hence adopt the equation

$$\nabla^2\chi = A_i|\chi|^{1-\frac{2}{\alpha}} \quad \text{in} \quad \mathscr{D}_i \quad \text{for} \quad i = 1,2,3,$$

which by setting $\chi(r,\theta) = (r/a)^\alpha f(\theta)$ becomes

$$f''(\theta)+\alpha^2 f(\theta) = A_i|f(\theta)|^{1-\frac{2}{\alpha}} \quad \text{for} \quad i = 1,2,3. \tag{3.2}$$

The solution to this equation has to vanish on the separatrices and must satisfy the total pressure continuity condition

$$\left\{\frac{B^2}{8\pi}+p\right\} = 0 \quad \text{on} \quad \partial\mathscr{D}_i \quad \text{for} \quad i = 1,2,3, \tag{3.3}$$

where the braces denote the jump of the enclosed quantity across the separatrices. When $r\to 0$, $B\to 0$ and therefore $\{B^2/8\pi\} = 0$ in the vicinity of $r = 0$. Hence according to (3.3), $\{P\} = 0$ and the magnetic field either is continuous or changes sign on each separatrix. Any solution of (3.2) must therefore satisfy $f'(\pi) = -f'(-\pi)$ in addition to $f(-\pi) = f(-\theta_1) = f(\theta_2) = f(\pi) = 0$. Without loss of generality assume that $f(\theta) \geqslant 0$ in the subdomain $\mathscr{D}_1$ and $f'(\theta_3) = 0$ with $-\theta_1 < \theta_3 < \theta_2$. Equation (3.2) is unchanged under the transformation $\theta\to-\theta$ which implies that $f(\theta_3-\theta) = f(\theta_3+\theta)$ in $\mathscr{D}_1$, and therefore $\theta_3 = \frac{1}{2}(\theta_2-\theta_1)$ with $f'(-\theta_1) = -f'(\theta_2)$. Similarly, it can be shown that $f'(-\pi) = -f'(-\theta_1)$ and $f'(\theta_2) = -f'(\pi)$ which proves that condition (3.3) is satisfied. The value of $f(\theta_3)$ can be absorbed into the constant A_1 so it can be assumed that $f(\theta_3) = 1$. Equation (3.2) is solved by the method of shooting. A value of A_1 is chosen and (3.2) is solved using the fourth-order Runge–Kutta method with initial conditions $f(0) = 1$, $f'(0) = 0$. If $f(-\frac{1}{2}(\theta_1+\theta_2)) = f(\frac{1}{2}(\theta_1+\theta_2))$ do not vanish then the value of A_1 is varied until this condition is fulfilled. This solution is then shifted by $\theta_3 = \frac{1}{2}(\theta_2-\theta_1)$ and $f(\theta)$ is determined in $\mathscr{D}_2$ and $\mathscr{D}_3$ by adjusting the values of A_2 and A_3 until $f(-\pi) = f(\pi) = 0$. This equation can be thus solved for every $\alpha \geqslant 2$ giving rise to a wide family of solutions.

The case $\alpha = 2$ has been solved analytically by Vainshtein (1990) and the solution is given by

$$\chi = \begin{cases} C(ax-y)(bx+y) & \text{for} \quad -\arctan b \leqslant \theta \leqslant \arctan a \\ C\dfrac{(a+b)}{a}y(ax-y) & \text{for} \quad \arctan a \leqslant \theta \leqslant \pi \\ C\dfrac{(a+b)}{b}y(y+bx) & \text{for} \quad -\pi \leqslant \theta \leqslant -\arctan b. \end{cases} \tag{3.4}$$

Hence in the case $\alpha = 2$ the current distribution is discontinuous across two of the separatrices and there is a current sheet on the third one. The strength of the current sheet for any α scales like $r^{\alpha-1}$. Figure 6(a, b) shows the similarity functions $f(\theta)$ corresponding to values $\alpha = 2, 3$. Figure 6(c, d) shows the plots of $\nabla^2\chi$ against χ for the above values of α. The values of the constants A_i corresponding to these two α values can be found in the figure 6 caption. Figure 6(e, f) shows the magnetic fields corresponding to the above values of α for $-\frac{1}{2} \leqslant x, y \leqslant \frac{1}{2}$.

This local analysis can be also applied to the behaviour of an equilibrium field close to a corner of angle 2ϕ on the boundary. If $2\phi < \pi$ then the solution is well behaved but for angles $2\phi > \pi$ there is no continuous solution with finite current on the corner's vertex.

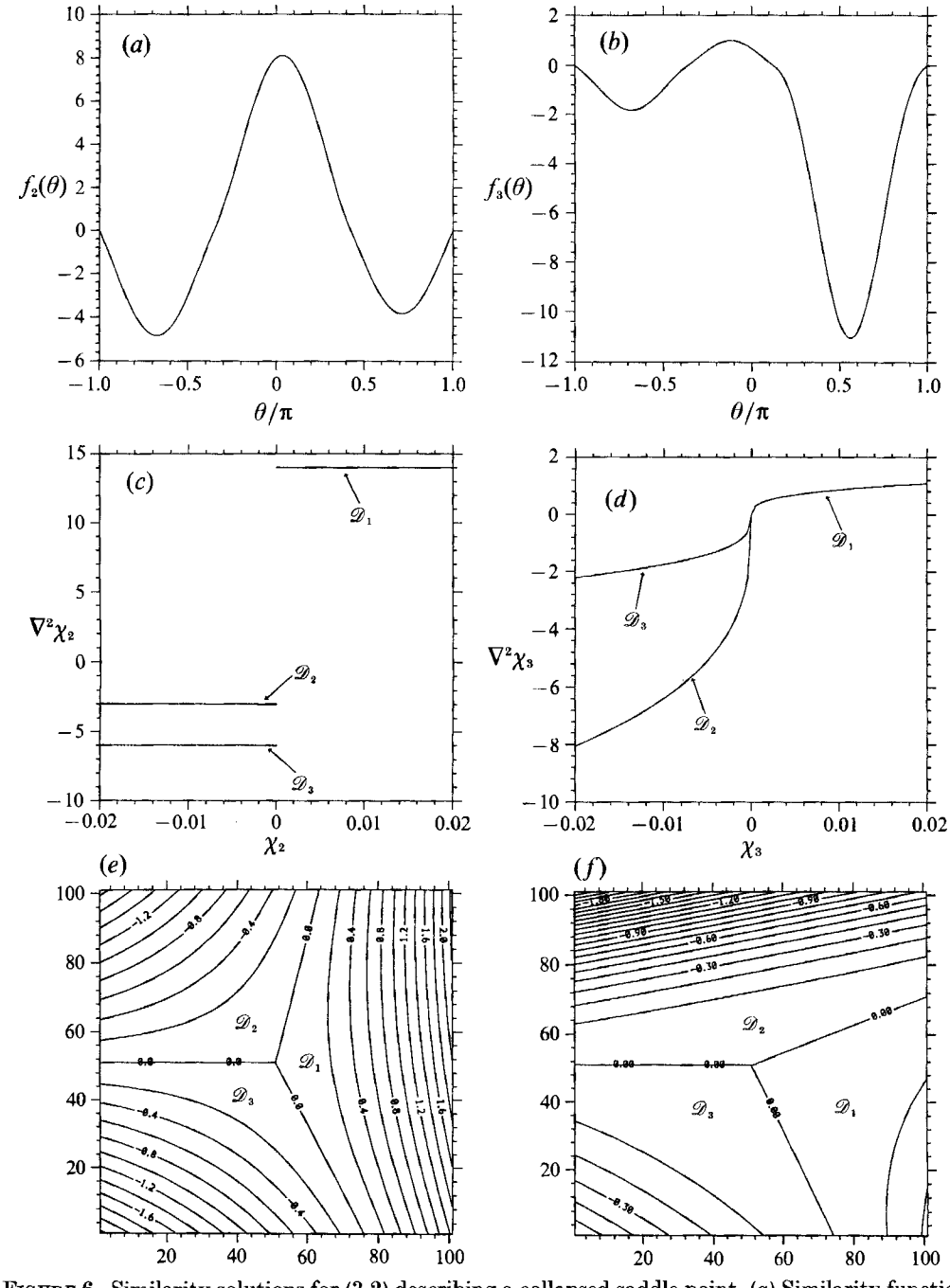

FIGURE 6. Similarity solutions for (3.2) describing a collapsed saddle point. (*a*) Similarity function $f(\theta)$ for $-\pi \leqslant \theta \leqslant \pi$ corresponding to the field in (3.4) with $C = 1$, $a = 4$ and $b = 2$. (*b*) Similarity function $f(\theta)$ for $-\pi \leqslant \theta \leqslant \pi$ corresponding to $\alpha = 3$. (*c*) $\nabla^2\chi$ against χ for $\alpha = 2$ with $A_1 = 14$, $A_2 = -3$ and $A_3 = -6$. (*d*) $\nabla^2\chi$ against χ for $\alpha = 3$ with $A_1 = 4$, $A_2 = -29.687$ and $A_3 = -8.134$. (*e*) The field in the unit square for $\alpha = 2$. (*f*) The field in the unit square for $\alpha = 3$.

3.2. *Numerical results*

Two numerical experiments were performed inside a unit square using again the relaxation equations (2.29). The discretization scheme used is the same as before and the Poisson equation was again solved using the IMSL fast Poisson solver. The variable-step-size fourth-order Runge–Kutta method proved to be the only reliable time-stepping routine. There are serious numerical problems in following the collapse of the saddle point to its asymptotic limit since the gradients in the magnetic field increase rapidly with time, and the routine used would stop execution as soon as the magnetic energy of the field started increasing due to numerical instabilities.

The first field considered is

$$\chi_0 = [y-\beta x-\tfrac{1}{2}(1-\beta)]\,[y+\beta x-\tfrac{1}{2}(1+\beta)]\,[\exp(5\sin\pi x)-1]\sin(\pi y)/W, \quad (3.5)$$

with $\beta = 0.3$ and W being a normalizing factor so that $|\chi_0|_{\max} = 1$. As can be seen in figure 7(*a*) this field divides the domain $\mathscr{D}$ in four subdomains and the plot of $\nabla^2\chi_0$ against χ_0 appears in figure 7(*c*). The relaxed field χ^{E} in figure 7(*b*) shows evidence of the collapse of the saddle point and the formation of a current sheet. Since the initial field scales like r^2 in all corners formed by $\boldsymbol{B}$-lines including the saddle point, we expect the equilibrium current to have a discontinuity across $\chi^{\mathrm{E}} = 0$ (on two of the separatrices). The high values of current for $\chi^{\mathrm{E}} = 0$ in the plot of $\nabla^2\chi^{\mathrm{E}}$ against χ^{E} in figure 7(*d*) give strong evidence of the formation of a current sheet on the third separatrix. Figure 7(*e*) shows the evolution of the field's magnetic energy during relaxation. Unfortunately the field energy has not completely settled down at the end of the calculation but it is impossible to continue further in time since the steep gradients in the magnetic field introduce numerical instabilities which make the energy increase. The surface plot of $\nabla^2\chi^{\mathrm{E}}$ in figure 7(*f*) also supports the assumption of the formation of a current sheet between the two strong magnetic eddies of the field.

The second field considered is

$$\chi_0 = \{[\exp(5\sin\pi y)-1]\exp(5\sin^2 2\pi x)\sin\pi x-[\exp(5)-1]\}/W, \quad (3.6)$$

with W being the usual normalizing factor. As figure 8(*a*) shows this field consists of two strong eddies inside the unit square which divide the domain $\mathscr{D}$ into three subdomains. Figure 8(*c*) is again the scatter of points of $\nabla^2\chi_0$ against χ_0 while the relaxed field is shown in figure 8(*b*). The structure of this field is called the rosette structure and is of great relevance to astrophysics (Vainshtein 1990). The initial field again scales like r^2 in all corners formed by $\boldsymbol{B}$-lines and we thus expect the equilibrium current to be discontinuous across $\chi^{\mathrm{E}} = 0$. The scatter of points near $\chi^{\mathrm{E}} = 0$ in figure 8(*d*) of $\nabla^2\chi^{\mathrm{E}}$ against χ^{E} underlines the difficulty of handling numerically a discontinuity of current and also hints at a persisting disequilibrium there. Figure 8(*e*) is the energy plot of this field during relaxation and the equilibrium current surface plot in figure 8(*f*) strongly supports the conclusion that a current sheet is being formed on one of the separatrices. We have not predicted the form of the equilibrium current distribution for these two fields using equation (2.13), since it is not possible to analytically calculate the signature functions corresponding to the initial fields. The reason is that the variables x and y cannot be separated in the initial field definitions (3.5), (3.6) and hence the signature functions cannot be written in a simple integral form. This is a completely practical problem though and in principle such a prediction can be made.

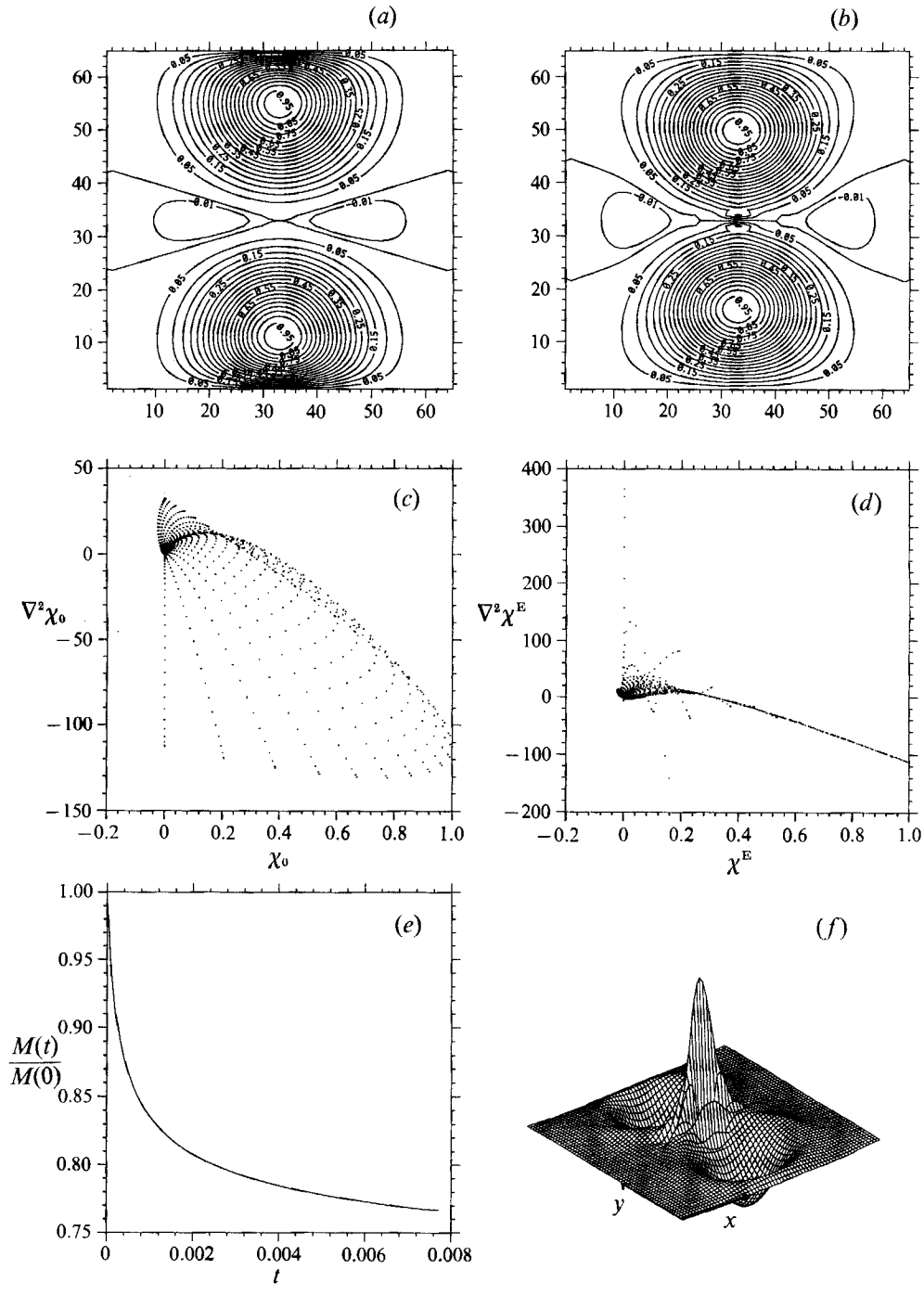

FIGURE 7. Magnetic relaxation results for field (3.5) (*a*) Initial $\boldsymbol{B}$-lines ($\chi_0 = \text{const.}$). (*b*) The numerically relaxed field χ^E. (*c*) $\nabla^2\chi_0$ against χ_0. This is just a scatter of points since χ_0 is not in equilibrium. (*d*) $\nabla^2\chi^E$ against χ^E giving evidence of a functional relationship between the equilibrium current $-\nabla^2\chi^E$ and the equilibrium flux function χ^E. The persistent scatter of points around $\chi^E = 0$ is a sign of disequilibrium in the vicinity of the saddle point. (*e*) Magnetic energy during relaxation of the field (the initial energy has been normalized to unity). (*f*) Surface plot of equilibrium current $-\nabla^2\chi^E$ with high values near the collapsed saddle point.

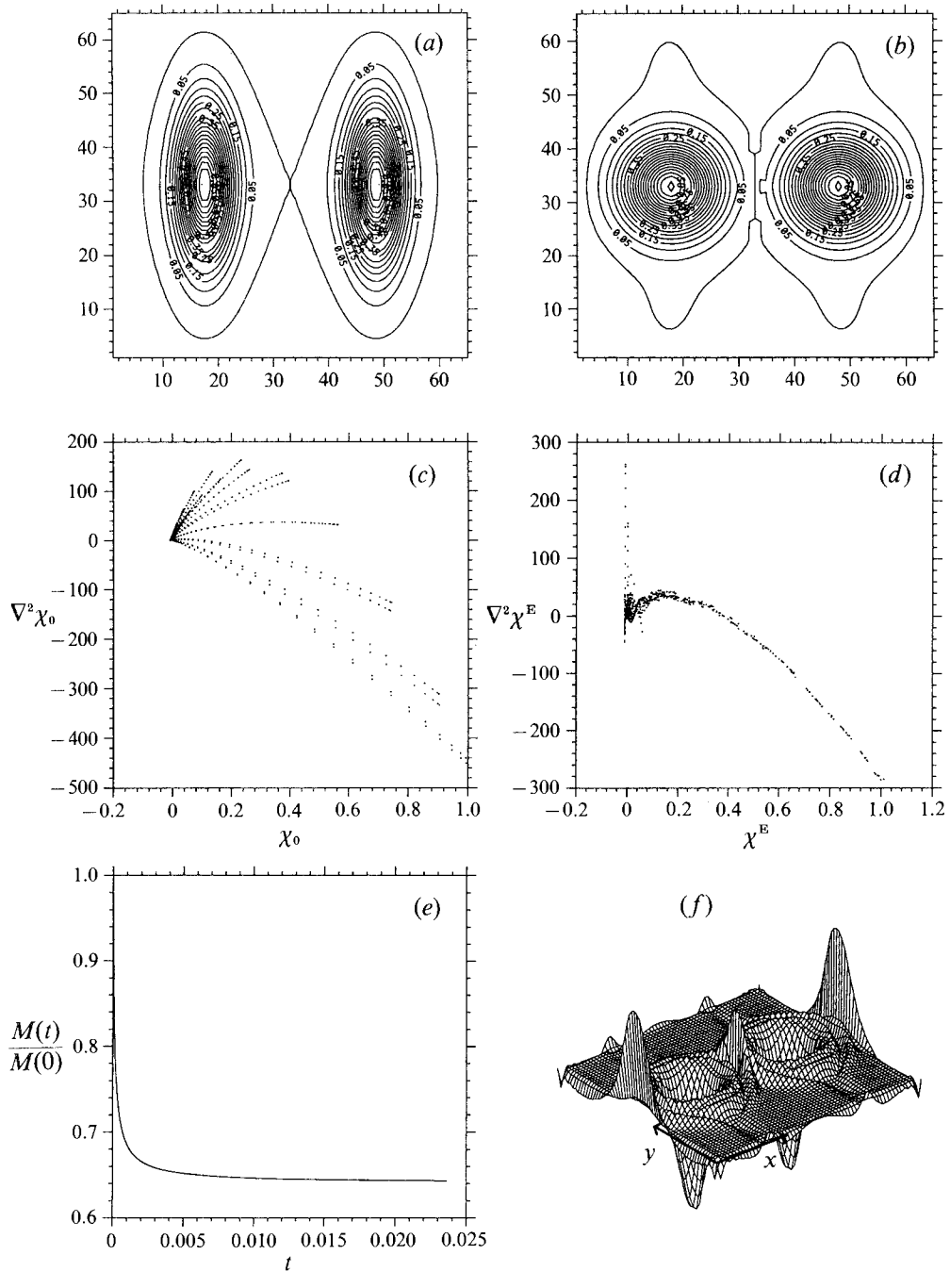

FIGURE 8. Magnetic relaxation results for field (3.6). (*a*)–(*f*) See caption for figure 7. The rosette structure emerging out of an initially continuous field may have some relevance to the coronal heating problem.

4. Conclusions

In this paper we have used a magnetic relaxation method to find a family of nonlinear two-dimensional magnetostatic equilibria. Using the exact analogy between a magnetostatic equilibrium and a steady Euler flow an equilibrium flux function χ^{E} can be replaced by an analogous stream function ψ^{E}. For the case of a flow with elliptic streamline topology we have seen that when the flow is strong close to the boundary of the domain then the steady Euler flow streamlines tend to align themselves with the boundary while for other cases they become more circular. When the initial field contains saddle points, the steady Euler flow obtained contains a number of vortex sheets which will presumably be unstable to a Kelvin–Helmholtz type of instability. Even so this suggests that the existence of vortex sheets might be a generic feature of steady Euler flows, which can be regarded as unstable fixed points in the function space in which unsteady solutions of the Euler equations evolve (Moffatt 1985). Any such unsteady solution is represented by a trajectory in this function space and very often it spends long periods of time close to such unstable fixed points. Study of such steady Euler flows of prescribed streamline topology can therefore give us valuable information about the structure of turbulence and their existence could not be inferred other than via the magnetic relaxation method.

Under two-dimensional magnetic relaxation every field line tries to minimize its length while preserving the area it encloses. This can therefore be treated as a variational problem with an infinity of constraints. This problem was formulated in terms of a Lagrange multiplier function $\lambda(\chi)$, which was shown to be a geometric property of the field lines. For the case of a finite-energy field containing a stationary elliptic point and extending to infinity we have shown that the minimum energy state is the one where all field lines have become concentric circles and that this state is topologically accessible from the original one. This state provides a useful reference state for understanding relaxation constrained by finite boundaries.

I wish to thank Professor H. K. Moffatt for helpful discussions and for reading earlier drafts of this paper. I am indebted to Dr S. I. Vainshtein for comments that have led to improvements in §3.1. I would also like to thank Dr K. Bajer, Dr B. J. C. Baxter, Dr L. Fradkin, Professor E. N. Parker and the referees for their advice and comments. The research described in this paper was partially performed in the Institute for Theoretical Physics in Santa Barbara which is supported by the National Science Foundation under NSF Grant PHY89-04035. I am grateful for financial support from Trinity College, Cambridge, and SERC.

REFERENCES

Arnol'd, V. I. 1974 The asymptotic Hopf invariant and its applications. In *Proc. Summer School in Differential Equations*. Erevan: Armenian SSR Academy of Science. (English transl. *Sel. Math. Sov.* **5**, 1986, 327–345.)

Arrowsmith, D. K. & Place, C. M. 1990 *An Introduction to Dynamical Systems*. Cambridge University Press.

Bajer, K. 1989 Flow kinematics and magnetic equilibria. PhD thesis, Cambridge University.

Batchelor, G. K. 1955 On steady laminar flow with closed streamlines at large Reynolds number. *J. Fluid Mech.* **1**, 177–190.

Boyd, J. P. & Ma, H. 1990 Numerical study of elliptical modons using a spectral method. *J. Fluid Mech.* **221**, 597–611.

FREEDMAN, M. H. 1988 A note on topology and magnetic energy in incompressible perfectly conducting fluids. *J. Fluid Mech.* **194**, 549–551.

ISERLES, A. & NØRSETT, S. P. 1991 *Order Stars*. Chapman & Hall.

MOFFATT, H. K. 1985 Magnetostatic equilibria and analogous Euler flows of arbitrary complex topology. Part 1. Fundamentals. *J. Fluid Mech.* **159**, 359–378.

MOFFATT, H. K. 1986 On the existence of localized rotational disturbances which propagate without change of structure in an inviscid fluid. *J. Fluid Mech.* **173**, 289–302.

MOFFATT, H. K. 1988 Generalised vortex rings with and without swirl. *Fluid Dyn. Res.* **3**, 22–30.

MOFFATT, H. K. 1990 Structure and stability of solutions of the Euler equations: a lagrangian approach. *Phil. Tran. R. Soc. Lond.* A **333**, 321–342.

PARKER, E. N. 1983 Heating of the outer solar atmosphere. In *Solar-Terrestrial Physics* (ed. R. L. Carovillano & J. M. Forbes), pp. 129–154. D. Reidel.

PARKER, E. N. 1987 Magnetic reorientation and the spontaneous formation of tangential discontinuities in deformed magnetic fields. *Astrophys. J.* **318**, 876–887.

PARKER, E. N. 1990 Spontaneous tangential discontinuities and the optical analogy for static magnetic fields VI. Topology of currents sheets. *Geophys. Astrophys. Fluid Dyn.* **53**, 43–80.

VAINSHTEIN, S. I. 1990 Cusp-points and current sheet dynamics. *Astron. Astrophys.* **230**, 238–243.